ON THE INTER-FIBRE FAILURE IN FIBRE REINFORCED COMPOSITES

Paolo A. Carraro, Marino Quaresimin, Michele Zappalorto

Department of Management and Engineering, University of Padova, Stradella San Nicola 3, Vicenza, Italy
Email: paoloandrea.carraro@unipd.it, marino.quaresimin@unipd.it, michele.zappalorto@unipd.it

Keywords: debonding, matrix failure, damage initiation, modelling, finite fracture mechanics

Abstract
In the present work a comprehensive analysis of interfibre failure in fibre reinforced composites is carried out, considering the phenomena of fibre/matrix debonding and matrix failure and highlighting the influence of the relevant material and geometrical parameters.
In particular it is shown the existence of a specific value of the fibre radius, R_f^*, which allows one to discern whether the fibre/matrix debonding is a stress-driven or an energy-driven interface process. At the same time the existence of a second limit value, R_{f0}, smaller than R_f^*, is argued, which provides the condition for the transition from interface to matrix failure.

1. Introduction

The static and fatigue failure of composite structures is the result of a multiscale and hierarchical damage process of which the first macroscopic evidence is often represented by the initiation of off-axis cracks, resulting from the accumulation of damage at the micro-scale in the form of matrix micro-cracking and fibre/matrix debonding. This makes the prediction of damage initiation at the micro-scale of basic importance to develop reliable failure criteria for this class of materials.
The initiation of off-axis cracks does not lead, necessarily, to catastrophic failure but it can affect the global behaviour of the composite (see, for a comprehensive literature review [1,2]) decreasing the stiffness and promoting the formation of other failure modes. This phenomenon is very complex to be described, especially because the local stress state in the matrix around a single fibre is multiaxial, so that a failure criterion needs to be used to combine local stress components.
Several investigations have been carried out in the past and recent literature to understand the matrix-dominated behaviour and the nature of matrix damage initiation at the micro-scale, thus assisting in the formulation of reliable criteria for matrix cracking. Experimental evidences [3-7] support the idea that under static and fatigue tensile loading the failure of the epoxy matrix is brittle, and damage in fibre reinforced epoxy off-axis plies was observed to initiate as micro-cracks between the fibres with an orientation normal to the local principal stress direction [7].
Differently, in the presence of a pure transverse tension or negligible local shear stresses, the local stress state at or close to the fibre–matrix interface is nearly hydrostatic [6,8]. Under such conditions, failure initiation was observed to occur in the form of matrix cavitation and consequent brittle cracking at the fibre–matrix interface.
These opposite behaviours suggest the use of a bi-parametric failure criterion to assess the onset of matrix cracks, according to which the Local Maximum Principal Stress (LMPS) should be used as effective strength parameter for loading conditions far enough from the pure transverse tension, where, instead, the Local Hydrostatic Stress (LHS) has to be used as representative of the driving force for damage evolution in the matrix [6].
Moving to the fibre/matrix debonding mechanism, interface investigation has been an important research field since the early days of fibre composites.

Excerpt from ISBN 978-3-00-053387-7

Several fracture criteria were proposed in the literature to predict the initiation of a debond crack, which can be effectively gathered into three main groups:
i) stress-based criteria;
ii) Cohesive Zone Models (CZMs);
iii) Finite Fracture Mechanics (FFM) based models.
Stress-based criteria are the most simple to implement and use and, for this reason, quite diffused. The major drawback of these criteria is that they are, by nature, not capable to account for the scale effect, meant as the influence of the fibre radius on the debonding process.
CZMs, frequently implemented in Finite Element codes, are based on the combined use of stress and energy criteria to govern the element separation in the numerical analysis. As a consequence, different from the stress based criteria, these methods are able to account for the influence of the fibre radius on the stress required for debond initiation.
The criteria related to the third group are based on the FFM approach, introduced by Leguillon [9], according to which two conditions (a stress criterion and an energy criterion) have to be simultaneously satisfied for the initiation of a crack. Mantič et al. [10] formulated a criterion for debond initiation for a fibre embedded in an infinite plate under remote transverse tension. According to this criterion the debonding stress depends on the interface strength, toughness and on the fibre radius. Later Mantič and Garcia [11] extended this approach to the case of biaxial transverse tension, thus introducing the effect of a through-the-thickness load in a composite laminate. Carraro and Quaresimin [12] adopted the FFM approach to formulate a criterion for debond initiation under a loading condition characterised by the presence of remote transverse and anti-plane shear stress, the latter corresponding to the in-plane shear stress for a composite ply. The model resulted in good agreement with the experimental data reported by Ogihara and Koyanagi [13].
The aim of the present work is to present a thorough analysis of the micro-scale interfibre failure in fibre reinforced composites. To this end, the competing phenomena of interface debonding and matrix failure are considered, highlighting the parameters which allow the actual damage scenario to be predicted.

2. Prediction of fibre/matrix debonding

2.1 A FFM-based model for fibre/matrix debonding

In the presence of a stress gradient, the FFM approach states that the failure of a solid under a (critical) remote stress level σ_c does not occur at a point but involves the sudden nucleation of a crack of finite length a_0, provided that the following two conditions are simultaneously satisfied [9]:

$$\begin{cases} \sigma(\sigma_c, a_0) = \sigma_R & (1.1) \\ \Delta G(\sigma_c, a_0) = G_c & (1.2) \end{cases}$$

Briefly:

- Eq. (1.1) represents a *stress condition*, according to which failure occurs whenever the stress over the length a_0 at least equates the material strength, σ_R;
- Eq. (1.2), instead, is the *energy criterion*, according to which the solid rupture occurs whenever the finite energy release rate ΔG reaches the critical energy release rate G_c. In other words, Eq. (1.2) requires that the released energy is equal to or larger than the energy barrier for the formation of two new fracture surfaces.

The two unknowns of the problem are the critical remote stress σ_c and the crack length a_0, which can be estimated by solving, in combination, Eq. (1.1) and Eq. (1.2).
With regard to the problem of the debonding of an isotropic fibre under a bi-axial stress state characterised by the presence of the remote transverse and anti-plane shear stresses, σ_2 and σ_6 (see Figure 1), Eq. (1) can be conveniently reformulated as it follows [12] (considering a unit thickness plate):

$$\begin{cases} \sigma_{eq}(\alpha_0) = \sqrt{\sigma_r^2(\alpha_0) + c \cdot \left[\tau_{r\theta}^2(\alpha_0) + \tau_{rz}^2(\alpha_0) \right]} = \sigma_R & (2.1) \end{cases}$$

Excerpt from ISBN 978-3-00-053387-7

$$\Delta U_{tot}(\alpha_0) = 2\alpha_0 \cdot R_f \cdot G_c \tag{2.2}$$

where:

- $2\alpha_0$ is the finite debonding crack angle;
- σ_r, $\sigma_{r\theta}$ and σ_{rz} are the stress components in the undamaged state, as evaluated at $r = R_f$ and $\theta = \alpha_0$ (see also figure 1);
- c is a multiaxiality parameter which represents the square of the ratio between the normal and shear interface strength;
- σ_R is the interface strength;
- ΔU_{tot} is the released energy;
- G_c is the critical interfacial energy release rate, which is regarded as a material property, independently of the mode mixity (see ref. [12] for a comprehensive discussion on this topic).

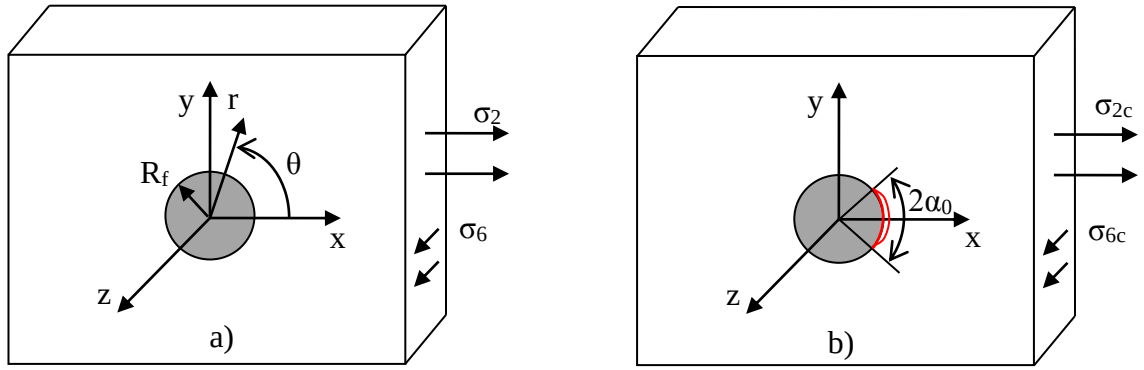

Figure 1. Fibre embedded in an infinite plate with a) pristine and b) partially debonded interface

In more explicit terms, Eqs. (2) can be re-written as it follows [30]:

$$\sigma_2 = \frac{\sigma_R}{\sqrt{k_{rr}(\alpha_0)^2 + c\left(k_{r\theta}(\alpha_0)^2 + \lambda_{12}^2 \cdot k_{rz}(\alpha_0)^2\right)}} \tag{3.1}$$

$$\sigma_2 = \sqrt{\frac{G_c}{R_f} \cdot \frac{2\alpha_0}{\left[\Omega_p \cdot \left(I_1(\alpha_0) + I_2(\alpha_0)\right) + \lambda_{12}^2 \cdot \Omega_a \cdot I_3(\alpha_0)\right]}} \tag{3.2}$$

where k_{ij} are the stress concentration factors around the fiber in the undamaged state [12] and λ_{12} is the anti-plane shear stress to the transverse stress ratio, $\lambda_{12}=\sigma_6/\sigma_2$. Instead, parameters I_j and Ω_j strictly depend on the relative crack opening and sliding displacements of a debond crack of angle 2α as well as on the stress fields in the undetached condition [12].

Thanks to Eqs. (3) the following relevant expression can be derived, of which the solution gives the initial crack angle α_0:

$$\frac{\frac{1}{2\alpha_0}\left[\Omega_p \cdot \left(I_1(\alpha_0) + I_2(\alpha_0)\right) + \lambda_{12}^2 \cdot \Omega_a \cdot I_3(\alpha_0)\right]}{k_{rr}(\alpha_0)^2 + c\left(k_{r\theta}(\alpha_0)^2 + \lambda_{12}^2 \cdot k_{rz}(\alpha_0)^2\right)} = \Gamma \tag{4}$$

where Γ is an interface parameter defined as:

$$\Gamma = \frac{1}{R_f}\frac{G_c}{\sigma_R^2} \tag{5}$$

Once α_0 is known from Eq. (4), the critical remote stress for debond initiation can be assessed either by Eq. (3.1) or (3.2). It is evident that the critical debonding stress strictly depends on:

- the interfacial strength σ_R;
- the interfacial toughness G_c;

Excerpt from ISBN 978-3-00-053387-7

- the fibre radius R_f;
- the biaxiality ratio λ_{12}.

2.2 Asymptotic behaviours for the critical debonding stress

As Γ vanishes, namely in the presence of large fibre radius and/or low values of the G_c/σ_R^2 ratio, the initial angle α_0 in Eqs. (3) tends to zero [12]. This corresponds to the physical situation where the initiation of a debond crack is fully controlled by the peak stress at the fibre pole. Under this condition, the critical stress can be assessed by the following equation:

$$\sigma_{2c} = \frac{\sigma_R}{\sqrt{k_{2,rr}^2 + c\left(k_{2,r\theta}^2 + \lambda_{12}^2 \cdot k_{6,rz}^2\right)}} \tag{6}$$

where the stress concentration factors $k_{i,km}$ relate the local stress σ_{km} at the fibre pole to the far applied stress σ_i.
Accordingly, introducing the following equivalent stress concentration factor k_{eq}:

$$k_{eq} = \sqrt{k_{2,rr}^2 + c \cdot \lambda_{12}^2 \cdot k_{6,rz}^2} \tag{7}$$

Eq. (6) can be re-written in the following form:

$$k_{eq} \frac{\sigma_{2c}}{\sigma_R} = 1 \tag{8}$$

Eq. (8) represents the *lower bound* for the critical stress.
Suppose now to consider the case c=0 and Γ tending to infinity, which corresponds to the physical situation of small fibre radii and/or large G_c/σ_R^2 ratios. Under these conditions, α_0 tends to the angle θ_0 for which the radial stress at the interface goes to zero [12]. Under these circumstances the initiation of a debond crack is fully controlled by the energy released during the process, ΔU_{tot}, and the critical stress can be assessed by the following equation (see Eq. 3.2):

$$k_{eq} \frac{\sigma_{2c}}{\sigma_R} = k_{eq} \sqrt{\frac{2\Gamma\theta_0}{\Omega_p \left[I_1(\theta_0) + I_2(\theta_0)\right] + \lambda_{12}^2 \, \Omega_a \, I_3(\theta_0)}} \tag{9}$$

The condition c=0 suffices to identify the asymptotic behaviour for the critical debonding stress for any value of c.
The resistance to fibre/matrix debonding is alternatively stress or energy-controlled, depending on whether the stress or the energy criterion provides the higher solution for the critical stress. Comparing Eq. (8) and Eq. (9), it is evident that, while Eq. (8) is independent of the fibre radius, Eq. (9) possesses a square root dependence on $1/R_f$. Accordingly, the two solutions intersect for a particular value of R_f, easy to be obtained equating the right-end side of Eqs. (8) and (9):

$$R_f^* = \frac{G_c}{\sigma_R^2} \cdot \frac{2 \cdot \theta_0 \cdot k_{eq}^2}{\left[\Omega_p \cdot \left(I_1(\theta_0) + I_2(\theta_0)\right) + \lambda_{12}^2 \cdot \Omega_a \cdot I_3(\theta_0)\right]} \tag{10}$$

R_f^* is the fibre radius providing the transition from an energy- to a stress-controlled behaviour.
From Eq. (10) it is evident that R_f^* depends on:

- the actual value of the stress concentration at the fibre pole, k_{eq}, as evaluated from Eq. (14);
- the interface strength, σ_R;
- the critical interfacial energy release rate, G_c
- the constituent elastic properties, through angle θ_0 and parameters I_j and Ω_j.

Substituting Eq. (20) into Eq. (18) one obtains:

$$k_{eq} \frac{\sigma_{2c}}{\sigma_R} = \sqrt{\frac{R_f^*}{R_f}} \tag{11}$$

Eq. (11) represents the asymptote of the critical debonding stress for large values of Γ.

Excerpt from ISBN 978-3-00-053387-7

A gradual transition between the two asymptotes can be obtained from the following simple equation:

$$k_{eq}\frac{\sigma_{2c}}{\sigma_R}=\sqrt[4]{\left(\frac{R_f^*}{R_f}\right)^2+1} \tag{12}$$

Eq.(12), which are valid independently of the material properties, interface strength and toughness and loading condition and do not require the numerical solution of Eq. (4) for the calculation of α_0, are compared to the complete solution from Eq. (3) in Figure 2, where a very satisfactory agreement can be noted.

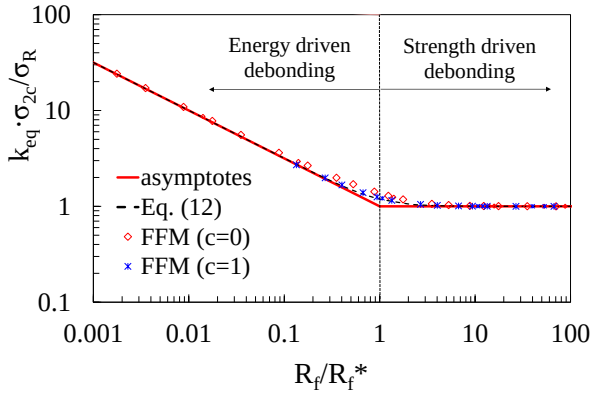

Figure 2. Asymptotic and simplified solutions compared to the FFM results for c = 0 and c = 1.

3. From interfacial debonding to matrix failure: upper limit for small values of the fibre radius

When the fibre radius R_f is much smaller than R_f^* and tends to zero, the solution for the critical debonding stress, Eq. (12), tends to an infinite σ_2 stress. This result is trivially wrong and is due to the fact that, reducing the fibre radius, the failure mode changes from interface failure to matrix failure.
As debated in the introduction, the initiation of matrix cracks is a very complex phenomenon to be described.
In particular, investigations in the literature suggest the use of a bi-parametric failure criterion to assess the onset of matrix cracks, according to which the Local Maximum Principal Stress (LMPS) should be used as effective strength parameter for loading conditions far enough from the pure transverse tension where, instead, Local Hydrostatic Stress (LHS) has to be used as representative parameter of the driving force for damage initiation and evolution in the matrix [6]. Notwithstanding this, in both cases the most critical point is the fibre pole, where the local stress state reads as:

$$\begin{Bmatrix}\sigma_{rr}\\ \sigma_{\theta\theta}\\ \sigma_{zz}\\ \sigma_{r\theta}\\ \sigma_{\theta z}\\ \sigma_{rz}\end{Bmatrix}=\begin{bmatrix}k_{2,rr} & 0\\ k_{2,\theta\theta} & 0\\ k_{2,zz} & 0\\ 0 & 0\\ 0 & 0\\ 0 & k_{2,rz}\end{bmatrix}\cdot\begin{Bmatrix}\sigma_2\\ \sigma_6\end{Bmatrix} \tag{13}$$

Accordingly, the local hydrostatic stress and the local maximum principal stress at the fibre pole, thought of as parameters governing matrix failure, can be written as:

$$LHS=\sigma_2\cdot\frac{k_{2,rr}+k_{2,\theta\theta}+k_{2,zz}}{3} \tag{14}$$

$$LMPS=\frac{\sigma_2}{2}\left[k_{2,rr}+k_{2,zz}+\sqrt{k_{2,rr}^2+4\cdot\lambda_{12}^2\cdot k_{6,rz}^2-2k_{2,rr}\cdot k_{2,zz}+k_{2,zz}^2}\right]. \tag{15}$$

respectively.

Excerpt from ISBN 978-3-00-053387-7

Matrix failure occurs when the following expression is verified by the remote stress:

$$k_{eq}\frac{\sigma_{2c}}{\sigma_R}=k_{eq}\frac{\sigma_{2m}}{\sigma_R} \tag{16}$$

where:

$$\sigma_{2m}=\min\left\{\sigma_{2,LHS},\sigma_{2,LMPS}\right\} \tag{17}$$

and:

$$\begin{aligned}\sigma_{2,LHS}&=\frac{3\cdot LHS_R}{\sigma_R}\cdot\frac{1}{k_{2,rr}+k_{2,\theta\theta}+k_{2,zz}}\\ \sigma_{2,LMPS}&=\frac{2\cdot LMPS_R}{\sigma_R}\cdot\frac{1}{k_{2,rr}+k_{2,zz}+\sqrt{k_{2,rr}^2+4\lambda_{12}^2k_{6,rz}^2-2k_{2,rr}k_{2,zz}+k_{2,zz}^2}}\end{aligned} \tag{18}$$

In other words, interface debonding and matrix failure are competing mechanisms, the latter occurring if the fibre radius is smaller than a limit value, R_{f0}, to be determined equating Eq. (16) to Eq. (12):

$$R_{f0}=R_f^*\cdot\left(\frac{\sigma_R}{k_{eq}\cdot\sigma_{2m}}\right)^2 \tag{19}$$

R_{f0} corresponds to the transition point between an interface-dominated and a matrix-dominated behaviour. It is evident that R_{f0} strictly depends on the matrix strength, $LMPS_R$ or LHS_R.

Accordingly, a comprehensive diagram can be drawn (Figure 3a) able to bridge the transition from one behaviour to the other. In particular, with reference to the schematic in Figure 3a, three distinct scenarios can be defined:

1. **Region I**, for fibre radii smaller than R_{f0} the most critical condition is the matrix strength, so that the apparent strength σ_{2c} is limited by σ_{2m};
2. **Region II**, for fibre radii comprised between R_{f0} and R_f^*, where the dominant failure mechanism is debonding. In this zone, the occurrence of debonding is conditioned by the interface fracture toughness (energy controlled mechanism);
3. **Region III**, for fibre radii larger than R_f^*, where the dominant failure mechanism is still debonding but, in this case, its occurrence depends on the interfacial strength (strength controlled mechanism).

It is important to note that, as mentioned in the previous section, in regions 2 and 3 conservative predictions for σ_{2c} are obtained using the asymptotes given by Eqs. (22). Differently, the use of asymptotic conditions to move from zone 1 and 2 will result in non-conservative estimation of the actual apparent strength, σ_{2c}. A safer and smooth transition between zone 1 and zone 2 can be achieved, instead, by means of the following equation:

$$k_{eq}\frac{\sigma_{2c}}{\sigma_R}=\left(\frac{R_f+R_{f0}}{R_f^*}\right)^{-1/2} \tag{20}$$

It is useful to underline that Eq. (20) is valid only in the close neighborhood of R_{f0}.

4. Application and discussion

Consider the glass fibre/epoxy system adopted by Ogihara and Koyanagi [13], characterised by the following elastic properties:

E_f = 72000 MPa ν_f = 0.22

E_m = 4280 MPa ν_m = 0.42

For this material, the fibre radius R_f was equal to 0.0085 mm, whereas the interface strength and toughness were estimated by Carraro and Quaresimin [12] taking advantage of the FFM criterion:

σ_R = 7.5 MPa G_c = 0.75 J/m^2

As far as the matrix strength is concerned the following typical values can be regarded as valid [8,12]:

Excerpt from ISBN 978-3-00-053387-7

LHS_R=46 MPa $LMPS_R$=70 MPa

In Ref. [13] several values for λ_{12} were considered. Using the relevant geometric and material data, it was possible to draw the comprehensive diagram introduced in the previous section for this material system, showing a very satisfactory agreement with experimental data (figure 3b). It is evident that, for all the conditions, the dominant failure mechanism is energy-controlled fibre/matrix debonding.

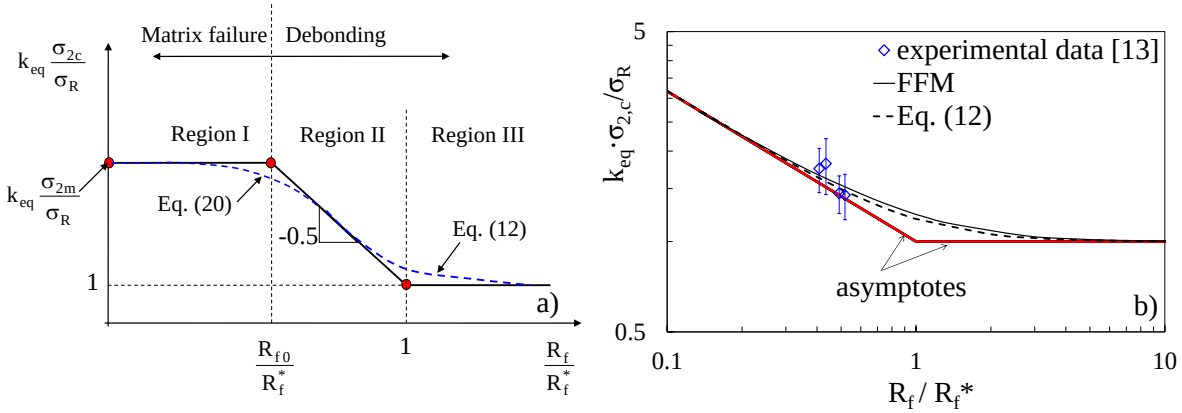

Figure 3. a) Schematic of normalised critical remote stress trend against the normalised fibre radius and b) comparison to experimental data from [13]

It is worth of being underlined that this conclusion has not a general validity, but it depends on the interfacial strength properties and on the local stress state close to the fibre. As an example, suppose to consider the same material as before, leaving unchanged all material parameters except for the interface toughness, G_c, which is chosen now to be equal to 10 J/m^2, as in the case of fibres treated by a coupling agent in the sizing by Zhang et al. [14]. As a consequence, one obtains:

R_f^* =1.26 mm R_{f0} =0.021 mm

for λ_{12} = 0,

R_f^* =0.20 mm R_{f0} =0.029 mm

for λ_{12} = 2 and c=0, and

R_f^* =1.658 mm R_{f0} =0.029 mm

for λ_{12} = 2 and c=1.

It is evident that for all cases the fibre radius, R_f=0.0085 mm, is lower than R_{f0}, so that the dominant failure mechanism is matrix failure.

5. Conclusions

A comprehensive analysis of the micro-scale interfibre failure in fibre reinforced composites was presented. It was underlined that interfacial debonding and matrix failure are competing damage mechanisms and the parameters which allow the actual damage scenario to be predicted were highlighted. Based on the results obtained, the following relevant conclusions can be drawn:

- for very small values of the fibre radius, less than a specific limit value R_{f0}, the interfiber failure is a matrix driven phenomenon. Beyond R_{f0}, a transition to an interface-driven failure is present;
- the existence of a second limit value, R_f^*, larger than R_{f0}, was noted, which allows one to distinguish whether the fibre/matrix debonding is a stress-driven or an energy-driven interface process.

References

[1] R. Talreja, C. Veer Singh, Damage and Failure of Composite Materials, *Cambridge University Press*, 2012.

Excerpt from ISBN 978-3-00-053387-7

[2] P.A. Carraro, M. Quaresimin, A stiffness degradation model for cracked multidirectional laminates with cracks in multiple layers, *Int. J. Solids Struct*. 58 (2015) 34-51.

[3] B.N. Cox, M.S. Dadkhah, W.L. Morris, J.G. Flintoff, Failure mechanisms of 3D woven composites in tension, compression, and bending, *Acta Metall. Mater*. 42 (1994) 3967 3984.

[4] M.Y. Shiino, L.M. De Camargo, M.O.H. Cioffi, H.C.J. Voorwald, E.C. Ortiz, M.C. Rezende, Correlation of microcrack fracture size with fatigue cycling on non-crimp fabric/RTM6 composite in the uniaxial fatigue test, *Compos Part B-Eng*. 43 (2012) 2244–2248.

[5] M. Quaresimin, P.A. Carraro, Damage initiation and evolution in glass/epoxy tubes subjected to combined tension-torsion fatigue loading, *Int J Fatigue* 63 (2014) 25–35.

[6] P.A. Carraro, M. Quaresimin, A damage based model for crack initiation in unidirectional composites under multiaxial cyclic loading, *Compos. Sci. Technol.* 99 (2014) 154–163.

[7] M. Quaresimin, P.A. Carraro, L. Maragoni, Damage evolution at the microscopic scale in off-axis plies under fatigue loading, to appear (2015).

[8] L.E. Asp, L.A. Berglund, R. Talreja, Prediction of matrix initiated transverse failure in polymer composites. *Compos. Sci. Technol*. 56 (1996) 1089-1097.

[9] D. Leguillon, Strength or toughness? A criterion for crack onset at a notch, *Eur. J. Mech. A-Solid* 21 (2002) 61-72.

[10] V. Mantič, Interface crack onset at circular cylindrical inclusion under a remote transverse tension. Application of a coupled stress and energy criterion, *Int. J. Solids Struct*. 46 (2009) 1287-1304.

[11] V. Mantic, I.G. García, Crack onset and growth at the fibre–matrix interface under a remote biaxial transverse load. Application of a coupled stress and energy criterion, *Int. J. Solids Struct*. 49 (2012) 2273–2290.

[12] P.A. Carraro, M. Quaresimin, Modelling fibre–matrix debonding under biaxial loading, *Compos. Part A-Appl. S*. 61 (2014) 33–42.

[13] S. Ogihara, J. Koyanagi, Investigation of combined stress state failure criterion for glass fiber/epoxy interface by the cruciform specimen method, *Compos. Sci. Technol*. 70 (2010) 143-150.

[14] H. Zhang, M.L. Ericson, J. Varna, L.A. Berglund, Transverse single-fibre test for interfacial debonding in composites: 1. Experimental observations, *Compos. Part A-Appl. S*. 28 (1997) 309-315.

Excerpt from ISBN 978-3-00-053387-7